P−*V*−*T*−*x* and Vapor−Liquid Equilibrium Properties of Pentafluoroethane (R125) + 1,1,1,3,3,3-Hexafluoroethane (R236fa) and 1,1,1,2-Tetrafluoroethane (R134a) + R236fa Systems Derived from Isochoric Measurements

Giovanni Di Nicola* and Fabio Polonara

Dipartimento di Energetica, Università di Ancona, 60100 Ancona, Italy

Roman Stryjek

Institute of Physical Chemistry, Polish Academy of Sciences, 01-224 Warsaw, Poland

P−*V*−*T*−*x* measurements were performed using a constant-volume apparatus for the pentafluoroethane (R125) + 1,1,1,3,3,3-hexafluoropropane (R236fa) and 1,1,1,2-tetrafluoroethane (R134a) + 1,1,1,3,3,3-hexafluoropropane (R236fa) systems, in a temperature range of (253−372) K and a pressure range of (113−2360) kPa. Experimental data were collected on three different compositions for each of the systems. Eight expansion series with a total of 121 data points and nine expansion series with 110 data points were performed, respectively, for the R125 + R236fa and R134a + R236fa systems, both within the vapor−liquid equilibrium (VLE) boundary and in the superheated vapor region. The data in the superheated vapor region were interpreted using tried and tested correlating methods for the second and third virial coefficients. The VLE parameters were derived by applying two methods: (1) The flash method enabled VLE parameters to be derived directly from *P*−*V*−*T*−*z* data within the VLE boundary by applying the Carnahan−Starling−De Santis (CSD) equation of state (EOS). (2) The dew-point method was based on dew-point evaluation by interpolating experimental *P*−*T* sequences. The resulting dew-point value was then used to derive VLE parameters, again using the CSD EOS. A comparison of the results emerging from these two methods, followed by the interpretation of the volumetric properties of the superheated vapor, confirmed their internal consistency.

Introduction

Severe deficiencies in the vapor−liquid equilibrium (VLE) and *P*−*V*−*T*−*x* data on refrigerant mixtures, and especially the more environmentally benign alternatives to 1,2-dichloro-1,1,2,2-tetrafluoroethane (R114), have become evident from an analysis of the scientific literature.

1,1,3,3,3,3-Hexafluoropropane (R-236fa) has a zero ozone depletion potential. In addition, because of its low global warming potential, this refrigerant is currently considered as one of the most promising substitutes for chlorine-containing compounds in high-temperature heat pumps, centrifugal chillers, and chemical blowing agents (for use in the manufacture of polyurethane and phenolic resin foams) and as a component in cleaning fluids, fire suppressants, and propellants.

A method which was developed for isochoric *P*−*V*−*T*−*z* data interpretation of binary systems has been described elsewhere.[1] Following studies on R236fa,[2] this is a report on the experimental results obtained from isochoric runs for two binary systems, i.e., pentafluoroethane (R125) + R236fa and 1,1,1,2-tetrafluoroethane (R134a) + R236fa. The experimental results roughly cover the temperature range from 253 to 372 K and a pressure range from 113 to 2360 kPa. In addition, they cover both the *P*−*V*−*T*−*x* and the VLE regions. Experimental VLE data from Bobbo et al.[3,4] were obtained at 303 and 323 K for the former and 283 and 303 K for the latter systems mentioned above. To our knowledge, the *P*−*V*−*T*−*x* data for the binary systems studied here have not been reported elsewhere in the literature.

* Corresponding author. Tel: +39-071-2204432. Fax: +39-071-2804239. E-mail: anfreddo@popcsi.unian.it.

Experimental Section

Reagents. R125 (CAS Reg. No. 354-33-6) and R134a (CAS Reg. No. 811-97-2) were donated by Ausimont Spa of Italy, and R236fa (CAS Reg. No. 690-39-1) was supplied by DuPont, Wilmington, DE. Their purity was checked by the authors using gas chromatography: the purities of R125 and R134a were better than 99.98%, while the purity of R236fa was better than 99.94%, based on the area fraction response of the thermal conductivity detector.

Experimental Setup. The experiment was carried out using the apparatus presented in Figure 1. It was used as described elsewhere,[5] so only the essential details are given here. The main element in the setup is a constant-volume spherical cell with a total capacity of (0.2548 ± 0.0003) dm^3, as shown by gravimetric calibration using water. The temperature was stabilized within ±5 mK using a thermostatic bath with proportional−integral−derivative (PID) control and was measured with a platinum resistance thermometer with an overall uncertainty of ±15 mK for temperatures above −5 °C and of ±30 mK for temperatures below −5 °C. The pressure was measured with a gas-lubricated dead weight pressure gauge to within ±0.5 kPa.

The experimental procedure has been described elsewhere;[1] hence, only changes in the preparation of the

10.1021/je000259x CCC: $20.00
Published on Web 02/17/2001

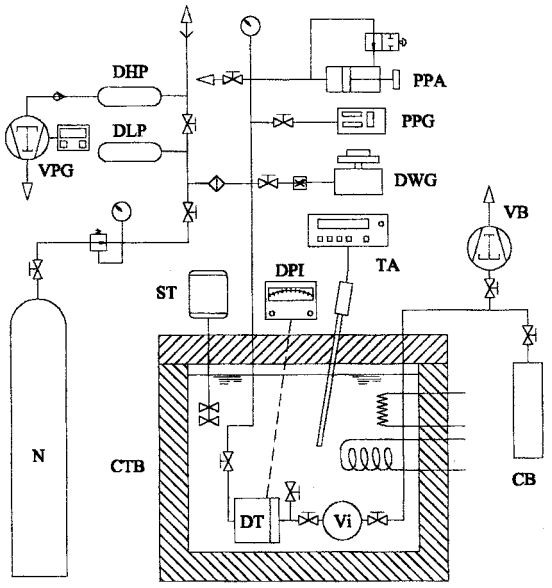

Nomenclature:

CB	Charging Bottle	PPA	Precision pressure controller (Ruska, mod. 3891)
CTB	Main thermostatic bath	PPG	Vibr. cylinder pressure gage (Ruska, mod. 6220)
DHP	High pressure expansion chamber	ST	Stirrer
DLP	Low pressure expansion chamber	TA	Platinum resistance Thermometer (Delta, PT100)
DPI	Electronic null indicator (Ruska, mod. 2461)	VB	Vacuum pump (Vacuubrand , mod. RZ2)
DT	Differential pressure transducer (Ruska, mod. 2413)	Vi	Constant volume spherical cell
DWG	Gas lubricated dead weight gage (Ruska, mod 2465)	VPG	Vacuum pump gage (Galileo, mod. OG510)
N	Nitrogen reservoir		

Figure 1. Schematic view of the experimental apparatus.

mixture are described here. The pure samples were first charged in different bottles and weighed with an analytical balance (uncertainty ±0.3 mg). Then, after the cell was evacuated, the bottles were discharged into the cell immersed in the bath. At the end of this operation, the bottles were weighed and the composition was found from the difference between the two weights. The dispersion of the mass inside the duct was estimated and subtracted from the total mass of the charge, and the uncertainty in the mass for this first charge was estimated to be lower than ±0.9 mg. The uncertainty for the mass yields an uncertainty for the molar fraction that can be estimated to be constantly within $\pm 3.3 \times 10^{-5}$. After a series of measurements and after the temperature of the sample is brought up to the superheated region, it was partially expanded and a new $P-T$ sequence was measured. The partially discharged sample was then weighed and subtracted from the total amount of the mixture, again taking the dispersion of the mass inside the duct into account. After the partial expansions, the uncertainty for the total mass was estimated to be lower than ±1.2 mg. Taking into account the uncertainty in the charged mass in the isochoric cell volume and in the pressure range, we estimated the uncertainty in molar volume of superheated vapor to be always lower than $\pm 9 \times 10^{-2}$ dm^3·mol^{-1}. A correction for thermal expansion and pressure distortion of the isochoric cell was considered, as reported elsewhere.[5] From the single uncertainties, the overall experimental uncertainty in terms of pressure, calculated using the laws of propagation, was estimated to be lower than ±0.6 kPa for measurements within the VLE boundary and lower than ±1.1 kPa in the superheated vapor region.

Results and Discussion

Information on the studied mixtures is given in Table 1, and the distribution of the $P-V-T-x$ measurements is shown in Figure 2. The data collected along the isochores are also given in Tables 2 and 3 for R125 + R236fa and in Tables 4 and 5 for R134a + R236fa. Tables 2 and 4 show the data collected within the VLE boundary, while Tables 3 and 5 show the findings pertaining to the superheated vapor region (data were assigned to the VLE or superheated region on the basis of $P-T$ slope analysis). The

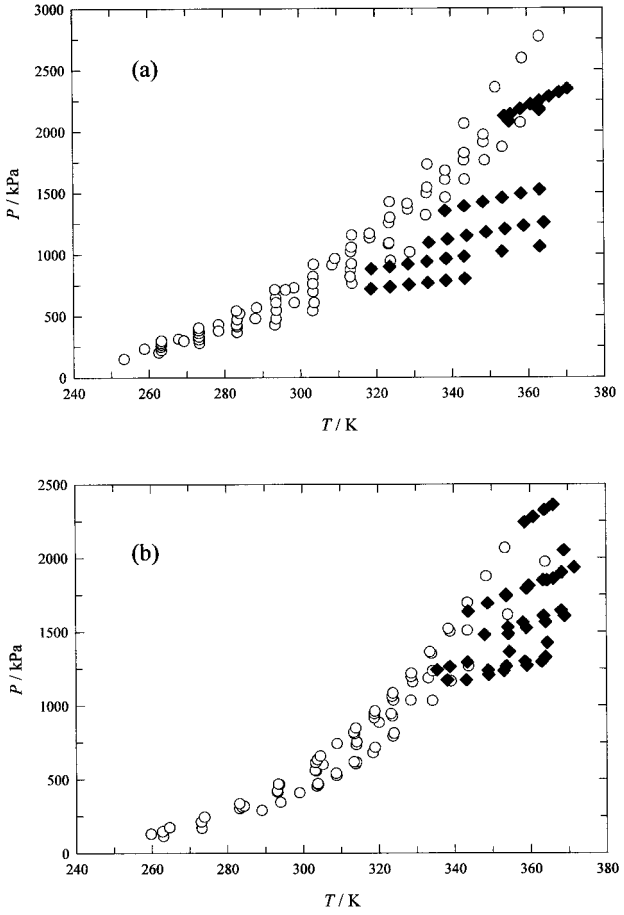

Figure 2. Distribution of the $P-V-T-x$ measurements for the R125 + R236fa system (a) and for the R134a + R236fa system (b): (○) data within the VLE boundary; (◆) data in the superheated vapor region. Notation of series: (○) 1st, (●) 2nd, (□) 3rd, (■) 4th, (△) 5th, (▲) 6th, (▽) 7th, (▼) 8th, and (◇) 9th.

Table 1. Compositions of the Investigated Systems

	no. of exptl points						
sample	total	VLE	vapor	m_1/g	m_2/g	x_1	$\sum n$
			R125 (1) + R236fa (2)				
1	8	2	6	4.174	7.269	0.421 10	0.0826
2	16	9	7	6.438	11.211	0.421 10	0.1274
3	14	13	1	13.947	24.288	0.421 10	0.2760
4	21	19	2	17.108	18.494	0.539 56	0.2642
5	16	8	8	7.210	6.620	0.579 78	0.1036
6	13	7	6	11.105	10.196	0.579 78	0.1596
7	21	13	8	18.954	17.402	0.579 78	0.2724
8	12	12	-	29.651	27.224	0.579 78	0.4261
			R134a (1) + R236fa (2)				
1	12	7	5	5.183	13.287	0.367 61	0.1382
2	10	6	4	6.654	17.058	0.367 61	0.1774
3	10	9	1	9.759	25.016	0.367 61	0.2602
4	13	8	5	8.878	8.245	0.616 07	0.1412
5	11	6	5	11.341	10.532	0.616 07	0.1804
6	11	6	5	13.802	12.817	0.616 07	0.2196
7	12	7	5	11.351	5.928	0.740 50	0.1502
8	16	10	6	15.578	8.135	0.740 50	0.2062
9	15	11	4	22.484	11.741	0.740 50	0.2976

Table 2. Experimental Data within the VLE Boundary for the R125 + R236fa System

sample	T/K	P/kPa	sample	T/K	P/kPa
1	293.25	427.5		348.40	1911.0
	303.22	541.2			
			5	263.15	248.5
2	253.31	149.8		269.19	296.7
	262.58	200.6		273.17	330.4
	273.28	278.1		278.35	378.9
	283.24	366.7		283.15	427.0
	293.54	477.0		288.10	478.8
	303.64	607.7		298.38	608.1
	313.61	761.1		313.15	817.6
	323.79	945.7			
	328.88	1016.5	6	263.22	265.4
				273.17	358.4
3	263.21	222.4		283.27	472.0
	273.16	306.5		293.58	607.8
	283.25	412.5		303.33	760.0
	293.62	545.8		313.52	920.8
	303.35	696.2		323.42	1089.7
	313.26	873.9			
	323.34	1081.9	7	263.15	278.4
	333.15	1316.8		273.14	381.8
	338.31	1460.2		283.94	520.0
	343.38	1606.0		296.07	711.6
	348.72	1761.2		309.17	964.1
	353.36	1871.0		313.49	1056.2
	358.22	2067.2		318.30	1167.6
				323.72	1297.4
4	258.78	232.5		328.28	1409.2
	263.17	269.7		333.50	1542.1
	267.81	313.3		338.32	1679.9
	273.19	369.9		343.37	1821.4
	278.34	430.2		348.42	1968.9
	283.37	495.4			
	288.40	566.8	8	263.28	297.1
	293.44	644.8		273.12	403.2
	298.33	727.6		283.11	541.3
	303.35	818.1		293.28	712.7
	308.42	913.3		303.48	917.9
	313.30	1020.5		313.62	1156.6
	318.34	1132.9		323.61	1424.3
	323.42	1253.1		333.60	1730.9
	328.35	1364.3		343.43	2060.3
	333.31	1495.2		351.61	2354.3
	338.25	1604.3		358.69	2591.7
	343.21	1761.2		363.19	2768.8

molar volume, V, of superheated vapor calculated from the equation

$$V = V_{iso}/n \tag{1}$$

where V_{iso} and n stand for the isochoric cell volume and the number of charged moles, is included in Tables 3 and 5 in relation to the experimental values.

VLE Derivation. For the VLE derivation from the isochoric data, we applied the Carnahan−Starling−De Santis (CSD) equation of state (EOS),[6] in which the pressure P is expressed as

$$P = \frac{RT}{V}\left[\frac{1 + Y + Y^2 - Y^3}{(1 - Y)^3}\right] - \frac{a}{V(V + b)} \tag{2}$$

where

$$Y = b/4V \tag{3}$$

In eq 2 R is the gas constant and T is the absolute temperature.

For pure compounds, the temperature dependence of parameters a and b in the CSD EOS is described by the following expressions:

$$a = a_0 \exp(a_1 T + a_2 T^2) \tag{4}$$

$$b = b_0 + b_1 T + b_2 T^2 \tag{5}$$

The following combining rules were used for the mixtures:

$$a = \sum_{N}^{i=1}\sum_{N}^{j=1} \xi_i \xi_j a_{ij} \tag{6}$$

$$b = \sum_{i=1}^{N} \xi_i b_i \tag{7}$$

where ξ_i is the mole fraction of the ith component in both the liquid and the vapor phase, and

$$a_{ij} = (1 - K_{ij})\sqrt{a_{ii} a_{jj}} \tag{8}$$

where K_{ij} is a dimensionless adjustable parameter for $i \neq j$ ($K_{ij} = K_{ji}$).

The corresponding coefficients, established from ref 7, are given in Table 6 for the reader's convenience.

(a) Flash Method. As a first approach to seeking the VLE, we applied the flash method (Reid et al.[8]), and each datum point within the VLE boundary was treated individually. In this step, the T, P, and z_i values were kept constant, and K_{12} was considered as an adjustable variable. By applying the flash method to the isochoric data, we also included the balance of the isochoric cell volume, as described elsewhere.[1] In addition, the composition and pressure at the bubble and dew points could be found for each datum set (T, P, z_i). The K_{12} values calculated in this way are presented graphically in Figures 3 and 4. Assuming its temperature independence, we found the average values of $K_{12} = -0.011\,527$ and $K_{12} = -0.008\,608$ for the R125 + R236fa and R134a + R236fa systems, respectively. The graphs show that the K_{12} values are slightly temperature-dependent, however. Assuming a linear temperature

Table 3. Experimental Data in the Superheated Vapor Region for the R125 + R236fa System

sample	T/K	P/kPa	V/dm³·mol⁻¹	sample	T/K	P/kPa	V/dm³·mol⁻¹
1	318.62	719.9	3.088		328.36	919.8	2.463
	323.62	736.6	3.089		333.37	940.9	2.463
	328.69	753.7	3.090		338.50	961.8	2.464
	333.62	769.5	3.091		343.16	980.9	2.464
	338.35	784.5	3.091		353.17	1021.2	2.466
	343.37	800.8	3.092		363.11	1060.6	2.467
2	333.93[a]	1095.3	2.004	6	338.18	1353.7	1.600
	338.85	1121.4	2.004		343.23	1389.1	1.600
	343.88	1149.5	2.005		348.18	1423.2	1.601
	349.02	1177.4	2.005		353.27	1457.9	1.601
	354.00	1203.8	2.006		358.23	1491.6	1.601
	358.94	1230.1	2.006		363.17	1524.2	1.602
	364.24	1257.1	2.007				
				7	353.97	2122.5	0.938
3	363.19	2169.7	0.926		355.60	2137.0	0.938
					358.16	2179.4	0.938
4	355.19	2080.1	0.967		360.92	2216.6	0.938
	363.19	2184.2	0.968		363.20	2246.4	0.938
					365.81	2281.2	0.939
5	318.72	882.1	2.462		368.45	2315.7	0.939
	323.56	899.6	2.462		370.57	2343.0	0.939

[a] Experimental points that were not considered in the final data reduction.

Table 4. Experimental Data within the VLE Boundary for the R134a + R236fa System

sample	*T*/K	*P*/kPa	sample	*T*/K	*P*/kPa
1	263.06	112.9		333.08	1186.4
	273.18	167.5			
	289.06	290.4	6	259.74	128.8
	303.62	453.6		284.38	318.8
	308.81	525.6		305.16	598.6
	313.91	603.3		320.04	885.7
	318.43	679.9		334.21	1233.9
				343.38	1508.0
2	293.99	343.9			
	304.00	464.7	7	283.20	334.3
	314.07	616.3		293.71	465.8
	323.75	793.2		303.31	613.9
	334.19	1032.9		313.54	809.1
	343.70	1266.3		318.76	917.1
				323.84	1036.0
3	299.09	408.0		328.94	1159.6
	303.87	470.4			
	308.73	541.1	8	264.67	173.0
	313.47	619.1		273.91	244.7
	319.00	716.3		293.48	468.0
	323.96	812.4		303.77	634.2
	339.06	1164.5		313.35	817.5
	354.02	1614.5		318.80	944.1
	363.91	1972.8		323.52	1060.7
				328.55	1194.8
4	262.81	145.7		333.92	1351.6
	273.09	211.5		338.83	1501.2
	283.25	301.8			
	293.23	413.4	9	304.53	657.4
	303.42	555.9		308.98	742.2
	314.05	734.6		313.94	847.5
	323.56	928.6		318.91	962.8
	328.44	1034.7		323.68	1084.0
				328.60	1219.2
5	283.84	310.8		333.47	1364.1
	293.20	422.1		338.38	1521.3
	303.17	560.9		343.45	1696.3
	314.17	753.4		348.41	1875.8
	323.24	943.9		353.37	2066.9

Table 5. Experimental Data in the Superheated Vapor Region for the R134a + R236fa system

sample	*T*/K	*P*/kPa	*V*/dm³·mol⁻¹	sample	*T*/K	*P*/kPa	*V*/dm³·mol⁻¹
1	343.11	1173.0	1.848		353.60	1749.5	1.164
	348.99	1209.6	1.848		359.65	1812.1	1.164
	352.99	1234.3	1.849		363.39	1850.3	1.164
	359.05	1270.4	1.849		368.30	1902.6	1.164
	362.99	1296.4	1.850		371.59	1935.9	1.165
2	354.22	1485.7	1.440	7	335.41	1241.5	1.695
	358.97	1525.6	1.440		338.77	1263.0	1.696
	364.00	1567.1	1.441		343.39	1294.0	1.696
	368.98	1607.4	1.441		354.49	1364.1	1.697
					364.46	1425.7	1.698
3	368.89	2052.1	0.983				
				8	343.63	1638.3	1.234
4	338.10	1173.2	1.807		348.77	1693.9	1.235
	348.87	1239.8	1.808		353.73	1742.5	1.236
	353.66	1266.8	1.809		359.00	1793.2	1.236
	358.58	1298.6	1.809		364.43	1848.8	1.237
	363.99	1328.1	1.810		366.10	1860.0	1.237
5	347.93	1481.4	1.416	9	358.56	2241.6	0.856
	354.09	1532.0	1.416		360.85	2279.2	0.856
	358.03	1563.4	1.416		363.81	2324.9	0.856
	363.50	1607.6	1.417		366.09	2359.9	0.856
	368.17	1644.5	1.417				

dependence, we found $K_{12} = -0.2406 \times 10^{-2} - 0.307\,05 \times 10^{-3}(T/\mathrm{K} - 273.15)$ and $K_{12} = -0.5057 \times 10^{-2} - 0.930\,77 \times 10^{-5}(T/\mathrm{K} - 273.15)$.

As a second step, found K_{12} values (with or without considering its temperature dependence) were used to reproduce all of the VLE data, holding T and z_i constant and taking pressure as the dependent variable. The deviations in pressure calculated in this way for each isochore are shown in Table 7, and the pressure deviations obtained when the temperature dependence of K_{ij} was considered are shown in Figures 5 and 6, respectively. However, it is evident from the results in Table 7 that the improvement in the data representation achieved using the temperature-dependent K_{12} is only marginal.

(*b*) *Interpolating Method.* The isochoric $P-T-z_i$ data also enable a dew-point derivation by interpolating the data representing the vapor state and the two-phase region. A discontinuity of the $(\partial P/\partial T)_{V,z_i}$ shows the transition from the two-phase to the single-phase (vapor) region, which coincides with the dew point. To find the dew-point ($P-T-y_i$) parameters numerically, the data above and below the dew point were fitted separately. The data within the VLE boundary were regressed using the Antoine type of equation:

$$\log P = A_1 - \frac{A_2}{A_3 + T} \tag{9}$$

We observed a random distribution of the deviations when they were plotted against temperature, and because they were independent of the charged mass and composition, they correspond mainly to the random error in equilibrium measurements. The data in the superheated vapor region were fitted to a second-degree polynomial:

$$P/\mathrm{kPa} = c_1 + c_2(T/\mathrm{K} - 273.15) + c_3(T/\mathrm{K} - 273.15)^2 \tag{10}$$

The two equations were then solved simultaneously for pressure and temperature, and the solution was adopted as the dew point. The findings are given in Table 8. After establishing the dew point, the $\varphi-\varphi$ method was used with the CSD EOS, enabling K_{12} and x_i to be found. In this way, we found mean $\bar{K}_{12} = -0.0330$ and $\bar{K}_{12} = -0.0120$ for the R125 + R236fa and R134a + R236fa systems, respectively.

When the K_{12} values obtained with the two methods were compared, we found some differences between them, which were, however, within the experimental errors and uncertainty for the extrapolation methods used. It is important to note here that, while extrapolation of two branches of the isochore was applied to find the temperature and pressure at dew point, the volumetric properties are not involved. Moreover, our data population in the superheated vapor region is less numerous than that for the VLE boundary, and a region in the proximity of the dew point is probably not very well represented by the equations used for the interpolation. For this reason, the results obtained with the interpolating method seem to be less accurate than the ones obtained with the flash method. Even if all of these factors contribute to the differences observed in $\bar{K}_{12}$ values emerging from these two methods, the consistency found between them is still quite good.

The VLE calculated with the CSD EOS and the K_{12} derived from our experimental data with the flash method were also compared with data in the literature,[3,4] and the deviations are shown in Table 9. Very good consistency is observed for the R134a + R236fa system; some systematic deviation is quite acceptable for the R125 + 236fa system considering that our method is not a direct one.

Considering the bubble-point behavior, both systems are zeotropic, the R125 + R236fa system shows slightly negative deviation from Raoult's law, and the R134a + R236fa system is almost ideal in terms of Raoult's law.

Table 6. a_i and b_i Coefficients of the CSD EOS and Parameters for R125, R134a, and R236fa

	compound		
parameter	R125	R134a	R236fa
a_0/kPa·dm^6·mol^{-2}	3427.9219	3582.1714	5812.833
a_1/K^{-1}	$-3.174\,613\,2 \times 10^{-3}$	$-2.811\,136\,2 \times 10^{-3}$	$-2.860\,835 \times 10^{-3}$
a_2/K^{-2}	$-1.757\,286\,1 \times 10^{-6}$	$-1.446\,788\,8 \times 10^{-6}$	$-1.409\,685 \times 10^{-6}$
b_0/dm^3·mol^{-1}	0.149 380 43	0.141 750 31	0.197 612 6
b_1/dm^3·mol^{-1}·K^{-1}	$-1.808\,510\,7 \times 10^{-4}$	$-1.627\,631\,0 \times 10^{-4}$	$-1.906\,306 \times 10^{-4}$
b_2/dm^3·mol^{-1}·K^{-2}	$-1.188\,133\,1 \times 10^{-7}$	$-0.628\,932\,64 \times 10^{-7}$	$-1.462\,412 \times 10^{-7}$
T_c/K	339.33	374.21	398.07
P_c/kPa	3629	4059	3200
V_c/dm^3·mol^{-1}	0.210 082	0.199 32	0.275 785
ω	0.303 667	0.318 263	0.377 82
μ/D	1.563	2.058	1.982

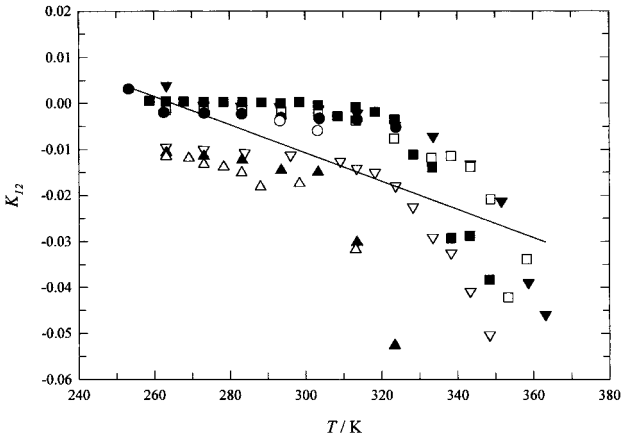

Figure 3. Scatter diagram of K_{12} values against temperature for the R125 + R236fa system. The line represents the linear temperature dependence of K_{12}. Symbols as in Figure 2.

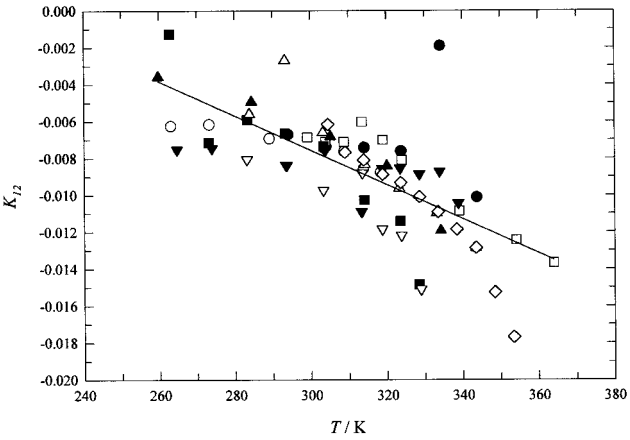

Figure 4. Scatter diagram of K_{12} values against temperature for the R134a + R236fa system. The line represents the linear temperature dependence of K_{12}. Symbols as in Figure 2.

***P*−*V*−*T*−*x* Modeling.** Experimental data in the superheated vapor region, within the reduced temperature ranges of 0.86−1.03 for the R125 + R236fa system and 0.89−0.98 for the R134a + R236fa system, were interpreted by means of the virial EOS. Expressed in terms of the inverse molar volume, the virial EOS takes the following form if it is truncated after the third term:

$$P = \frac{RT}{V}\left(1 + \frac{B}{V} + \frac{C}{V^2}\right) \tag{11}$$

where B and C are the second and third virial coefficients. For mixtures, the second and third virial coefficients are expressed through the relations

$$B = \sum_{i=1}^{N}\sum_{j=1}^{N} x_i x_j B_{ij} \tag{12}$$

$$C = \sum_{i=1}^{N}\sum_{j=1}^{N}\sum_{k=1}^{N} x_i x_j x_k C_{ijk} \tag{13}$$

Given that our isochoric experimental method does not allow points to be measured along isotherms and given the limited pressure and temperature ranges of our data, we chose to compare our experimental pressure and molar volume data with the correlating methods available in the literature. From among the more general correlations describing second virial coefficients, we opted for the one proposed by Tsonopoulos;[9,10] as for the third virial coefficients, we used the correlation proposed by Orbey and Vera.[11]

The Tsonopoulos correlation for the second virial coefficient takes the form

$$B_{ij} = RT_{ij}^{c}/P_{ij}^{c}(F_1 + F_2 + F_3) \tag{14}$$

where

$$F_1 = 0.1445 - 0.330/T_R - 0.1385/T_R^{2} - 0.0121/T_R^{3} - 0.000607/T_R^{8} \tag{15}$$

$$F_2 = \omega_{ij}(0.0637 + 0.331/T_R^{2} - 0.423/T_R^{3} - 0.008/T_R^{8}) \tag{16}$$

$$F_3 = -0.000214\mu_R/T_R^{6} \tag{17}$$

and

$$T_R = T/T_{ij}^{c} \tag{18}$$

$$T_{ij}^{c} = (T_i^{c}T_j^{c})^{1/2}(1 - L_{ij}) \tag{19}$$

$$\mu_R = 9.896 \times 10^{2}\mu_i\mu_j P_{ij}^{c}/T_i^{c}T_j^{c} \tag{20}$$

$$\omega_{ij} = (\omega_i + \omega_j)/2 \tag{21}$$

$$P_{ij}^{c} = \frac{4T_{ij}^{c}(P_i^{c}\nu_i^{c}/T_i^{c} + P_j^{c}\nu_j^{c}/T_j^{c})}{(\nu_i^{c1/3} + \nu_j^{c1/3})^3} \tag{22}$$

L_{ij} is the only adjustable parameter per binary system ($L_{ij} = L_{ji}$); for a one-component system, $L_{ij} = 0$.

Table 7. Deviations in Pressure, as ΔP (%), from the Fit of the Data within the VLE Boundary: (a) Disregarding the Temperature Dependence of K_{12}; (b) Considering a Linear Temperature Dependence of K_{12}

	a		b			a		b	
R125 + R236fa	bias	AAD	bias	AAD	R134a + R236fa	bias	AAD	bias	AAD
1	0.98	0.98	0.76	0.76	1	0.38	0.39	−0.13	0.25
2	2.40	2.40	0.68	0.97	2	0.48	0.48	0.48	0.48
3	1.45	1.73	1.29	1.43	3	0.17	0.42	0.29	0.29
4	1.64	2.46	1.14	1.55	4	0.24	0.79	−0.14	0.41
5	−0.61	0.61	−2.16	2.16	5	0.36	0.59	0.26	0.28
5	0.36	0.59	0.26	0.28	5	0.36	0.59	0.26	0.28
6	−0.76	0.83	−2.46	2.46	6	0.24	0.74	0.06	0.23
7	−1.13	1.33-	1.08	1.17	7	−0.25	0.30	−0.43	−0.43
8	0.97	2.10	1.23	1.59	8	−0.01	0.16	−0.06	0.30
					9	−0.30	0.43	−0.10	0.24
average	0.69	1.75	0.11	1.54	average	0.10	0.46	0.00	0.32

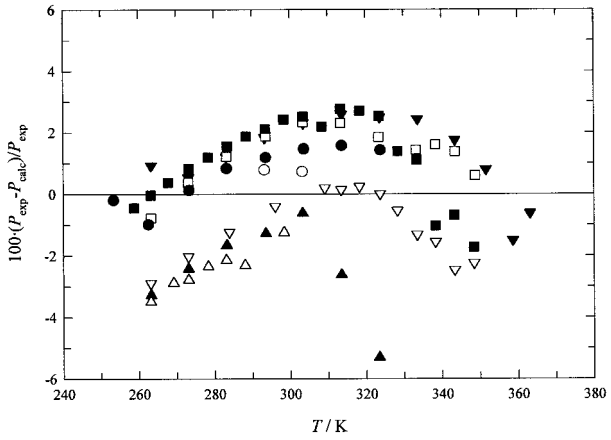

Figure 5. Deviations in pressure against temperature, calculated assuming the temperature dependence of K_{12} for the R125 + R236fa system. Symbols as in Figure 2.

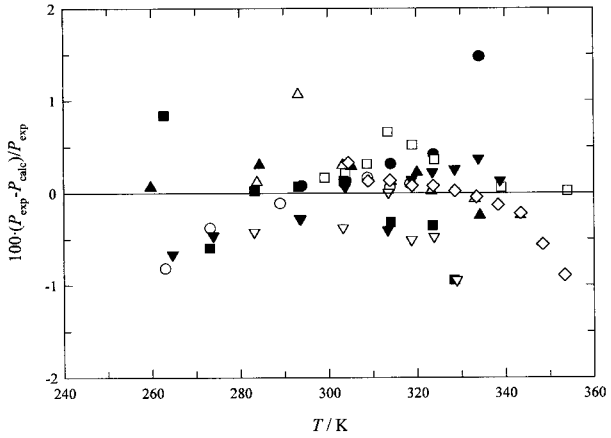

Figure 6. Deviations in pressure against temperature, calculated assuming the temperature dependence of K_{12} for the R134a + R236fa system. Symbols as in Figure 2.

The Orbey and Vera correlation for the third virial coefficient takes the form

$$C_{ij} = \frac{(RT_{ij}^{c})^2}{P_{ij}^{c2}}(f_1 + \omega_{ij} f_2) \tag{23}$$

where

$$f_1 = 0.01407 + 0.02432/T_R^{2.8} - 0.00313/T_R^{10.5} \tag{24}$$

$$f_2 = -0.02676 + 0.0177/T_R^{2.8} + 0.04/T_R^{6} - 0.00228/T_R^{10.5} \tag{25}$$

and

$$C_{ijk} = (C_{ij}C_{ik}C_{jk})^{1/3} \tag{26}$$

The cross-parameters that appear are defined as in the Tsonopoulos equations. In these methods, only one adjustable parameter (L_{ij}) appears for each binary system, being needed to describe the course of the critical temperature of the mixtures. The parameters required were taken from ref 12, and they are included in Table 6. The value of the binary interaction parameter (L_{ij}) needed to calculate the critical temperature of mixtures was not available in the literature. To overcome this problem, we used several L_{ij} values and found that the differences in the results were limited over quite a wide range of the attempted values; we ultimately adopted $L_{12} = 0.025$ for the binary systems. Considering the volumetric properties, eq 11 was rewritten as

$$(PV/RT - 1)V = B + C/V \tag{27}$$

The deviation in molar volume was calculated for each ith point, taking experimental P, T, V, and x values, as follows:

$$\Delta V = (PV/RT - 1)V - (B + C/V) \tag{28}$$

in which B and C were calculated using eqs 12−26. The absolute average deviations (AAD) and bias in volume were calculated as

$$\mathrm{AAD} = \sum_{i=1}^{N} \mathrm{abs}(\Delta V_i)/N \tag{29}$$

and

$$\mathrm{bias} = \sum_{i=1}^{N} \Delta V_i/N \tag{30}$$

In a similar way, we calculated deviations in pressure for each ith point, taking experimental P, T, V, and x_i values:

$$\Delta P = 100(P_{\mathrm{calc}} - P_{\mathrm{exp}})/P_{\mathrm{exp}} \tag{31}$$

where

$$P_{\mathrm{calc}} = [RT/V(1 + B/V + C/V^2)] \tag{32}$$

The AAD and bias deviations in pressure are defined in eqs 29 and 30, respectively.

Deviations in volume and pressure are given in Table 10 and illustrated in Figures 7 and 8 for the R125 + R236fa system and in Figures 9 and 10 for the R134a + R236fa system. There is evidence of a slight but systematic trend

Table 8. Dew-Point Parameters for the Studied Systems[a]

R125 + R236fa	*T*/K	*P*/kPa	K_{12}	x_1	R134a + R236fa	*T*/K	*P*/kPa	K_{12}	x_1
2	330.19	1074.1	−0.0084	0.20957	1	340.81	1159.1	−0.0134	0.25663
5	316.57	872.2	−0.0337	0.32149	2	349.82	1448.2	−0.0082	0.26331
6	336.32	1340.6	−0.0868	0.38203	4	332.56	1138.1	−0.0113	0.47442
7	352.30	2095.6	0.0525	0.41002	5	341.90	1431.5	−0.0118	0.48762
					6	349.39	1706.0	−0.0120	0.49849
					7	330.82	1210.7	−0.0123	0.61251
					8	342.48	1626.5	−0.0075	0.63024
					9	356.85	2213.5	−0.0159	0.64842
average			−0.0330		average			−0.0120	

[a] *T* and *P* were found by interpolation, and K_{12} and x_1 were found from the CSD EOS.

Table 9. Calculated Deviations in Pressure at $x_1 = 0.5$ for the Studied Systems (K_{12} Calculated with the Flash Method)

		K_{12}		
system	*T*/K	this work	lit.[4]	d*P* (%)[a]
R125 + R236fa	303.19	−0.011 68	0.000 23	1.60
	323.26	−0.017 85	−0.000 68	2.16
R134a + R236fa	283.62	−0.006 03	−0.006 38	−0.05
	303.65	−0.007 90	−0.007 31	0.09

[a] $dP = 100(P_{lit} - P_{our})/P_{lit}$.

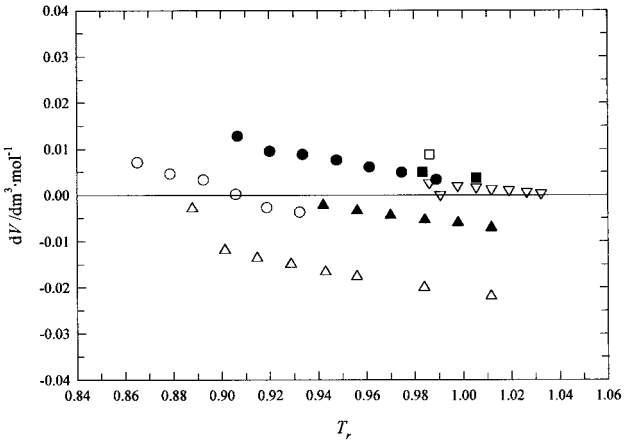

Figure 7. Deviations in molar volume against reduced temperature for the R125 + R236fa system, for data in the superheated vapor region. Symbols as in Figure 2.

in the deviations when results are compared among isochores, though there are no overall systematic deviations observable. This means that we probably underestimated the uncertainty in the isochoric cell volume calibration and overestimated the uncertainty in the charged mass, suggesting that some improvement in our charging procedure might improve the accuracy of our measurements. In general, however, the deviations produced by these matched models are rather small, within ±0.015 $dm^3 \cdot mol^{-1}$ in molar

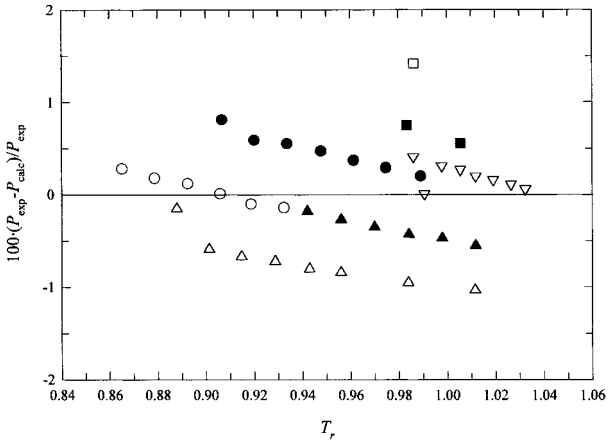

Figure 8. Deviations in pressure against reduced temperature for the R125 + R236fa system, for data in the superheated vapor region. Symbols as in Figure 2.

volume for both systems and 0.43% and 1.11% in pressure for the R125 + R236fa and R134a + R236fa systems, respectively. The contributions to the deviations that come from the third virial coefficient for our reduced temperature and pressure ranges are small, no more than a few percent. (As shown elsewhere,[13] the respective models for correlating the second and third virial coefficients proposed more recently by Weber[14,15] give very similar results, with differences coming well within the uncertainty of our experimental data; for the sake of brevity, they are consequently not included in this study).

Conclusions

The isochoric method we applied enabled the derivation of both VLE parameters and $P-V-T-x_i$ data from one run of experiments over a wide temperature range (more than 100 K). Although the VLE parameters within the VLE boundary were not obtained from direct VLE measurements, inasmuch as they could be compared with the literature, they showed quite good consistency. Moreover, the pressure deviations from the fit are somewhat ran-

Table 10. Deviations in Pressure (Eq 31) and in Molar Volume (Eq 28) for the $P-V-T-x$ Data in the Superheated Vapor Region

	Δ*P* (%)		Δ*V*/$dm^3 \cdot mol^{-1}$			Δ*P* (%)		Δ*V*/$dm^3 \cdot mol^{-1}$	
R125 + R236fa	bias	AAD	bias	AAD	R134a + R236fa	bias	AAD	bias	AAD
1	0.058	0.138	0.001	0.004	1	0.392	0.392	0.006	0.006
2	0.469	0.469	−0.001	0.014	2	0.933	0.933	0.010	0.010
3	1.420	1.420	0.009	0.009	3	1.710	1.710	0.011	0.011
4	0.650	0.650	0.004	0.004	4	−1.944	1.944	−0.027	0.027
5	−0.719	0.719	−0.015	0.015	5	−1.012	1.012	−0.011	0.011
6	−0.375	0.375	−0.005	0.005	6	−0.218	0.262	−0.002	0.002
7	0.191	0.191	0.001	0.001	7	−0.840	0.840	−0.011	0.011
average	0.003	0.431	−0.002	0.007	8	1.383	1.383	0.013	0.013
					9	2.093	2.093	0.012	0.012
					average	0.100	1.110	−0.001	0.011

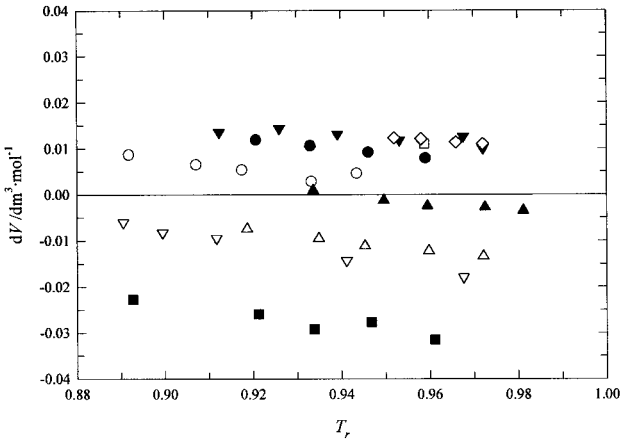

Figure 9. Deviations in molar volume against reduced temperature for the R134a + R236fa system, for data in the superheated vapor region. Symbols as in Figure 2.

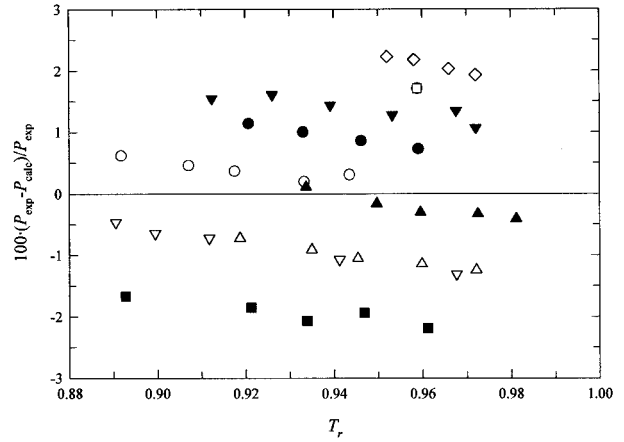

Figure 10. Deviations in pressure against reduced temperature for the R134a + R236fa system, for data in the superheated vapor region. Symbols as in Figure 2.

domly distributed if they are plotted against temperature, and being within about 1% on average, they are quite satisfactory. Considering the $P-V-T-x_i$ results, even though virial coefficients were not derived, a satisfactory volumetric and pressure representation of our data was found by applying the correlating methods recommended in the literature.

Acknowledgment

This work has been supported by the European Union as part of the Joule Project within the IV Framework for RTD and by the Italian Ministero dell'Università e della Ricerca Scientifica e Tecnologica.

Literature Cited

(1) Di Nicola, G.; Giuliani, G.; Passerini, G.; Polonara, F.; Stryjek, R. Vapor−liquid-equilibrium (VLE) properties of R-32 + R-134a system derived from isochoric method. *Fluid Phase Equilib.* **1998**, *153*, 143−165.

(2) Di Nicola, G.; Giuliani, G.; Polonara, F.; Stryjek, R. Saturated pressure and $P-V-T$ measurements for 1,1,1,3,3,3-hexafluoropropane (R-236fa). *J. Chem. Eng. Data* **1999**, *44*, 696−700.

(3) Bobbo, S.; Stryjek, R.; Elvassore, N.; Bertucco, A. A recirculation apparatus for vapor−liquid equilibrium measurements of refrigerants. *Fluid Phase Equilib.* **1998**, *150*, 343−352.

(4) Bobbo, S.; Camporese, R.; Stryjek, R. Vapor−liquid equilibria for difluoromethane (R32) + and pentafluoroethane (R125) + 1,1,1,3,3,3-hexafluoropropane (R236fa) at 303.2 and 323.3 K. *J. Chem. Eng. Data* **1999**, *44*, 348−352.

(5) Giuliani, G.; Kumar, S.; Polonara, F. A constant volume apparatus for vapour pressure and gas phase $P-v-T$ measurements: validation with data for R22 and R134a. *Fluid Phase Equilib.* **1995**, *109*, 265−279.

(6) De Santis, R.; Gironi, F.; Marrelli, L. Vapor−liquid equilibrium from a hard-sphere equation of state. *Ind. Eng. Chem. Fundam.* **1976**, *15*, 183−189.

(7) Huber, M.; Gallagher, J.; McLinden, M. O.; Morrison, G. *NIST thermodynamic properties of refrigerants and refrigerant mixtures database (REFPROP)*, version 5.0; Thermophysics Division, National Institute of Standards and Technology: Gaithersburg, MD, 1996.

(8) Reid, R. C.; Prausnitz, J. M.; Poling, B. E. *The Properties of Gases & Liquids*; McGraw-Hill: New York, 1987.

(9) Tsonopoulos, C. An empirical correlation of second virial coefficients. *AIChE J.* **1974**, *20*, 263−272.

(10) Tsonopoulos, C. An empirical correlation of second virial coefficients. *AIChE J.* **1975**, *21*, 827−829.

(11) Orbey, H.; Vera, J. H. Correlation for the third virial coefficient using T_c, P_c and ω as parameters. *AIChE J.* **1983**, *29*, 107−113.

(12) McLinden, M. O.; Klein, S. A.; Lemmon, E. W.; Peskin, A. P. *NIST thermodynamic and transport properties of refrigerants and refrigerant mixtures (REFPROP)*, version 6.01; Physical and Chemical Properties Division, National Institute of Standards and Technology: Gaithersburg, MD, 1998.

(13) Polonara, F.; Stryjek, R.; Di Nicola, G. Virial coefficients from isochoric measurements for R236fa, R236ea, R32 + R236ea, R125 + R236fa, and R134a + R236fa systems. Paper presented at the 20th International Congress of Refrigeration, IIR/IIF, Sydney, Australia, Sept 1999.

(14) Weber, L. A. Estimating the virial coefficients of small polar molecules. *Int. J. Thermophys.* **1994**, *15*, 461−482.

(15) Weber, L. A. Predicting the virial coefficients and thermodynamic properties of a multicomponent mixture with application to the ternary mixture of CH_2F_2 + CF_3CHF_2 + CF_3CH_2F. *Int. J. Thermophys.* **1997**, *18*, 161−172.

Received for review August 8, 2000. Accepted December 4, 2000.

JE000259X